Precise Measurement of the Pion Axial Form Factor in the $\pi^+ \to e^+ \nu\gamma$ Decay

E. Frlež,[1,*] D. Počanić,[1,†] V. A. Baranov,[3] W. Bertl,[2] M. Bychkov,[1] N. V. Khomutov,[3] A. S. Korenchenko,[3] S. M. Korenchenko,[3] T. Kozlowski,[4] N. P. Kravchuk,[3] N. A. Kuchinsky,[3] W. Li,[1] R. C. Minehart,[1] D. Mzhavia,[3] B. G. Ritchie,[6] S. Ritt,[2] A. M. Rozhdestvensky,[3] V. V. Sidorkin,[3] L. C. Smith,[1] I. Supek,[7] Z. Tsamalaidze,[5] B. A. VanDevender,[1] E. P. Velicheva,[3] Y. Wang,[1] H.-P. Wirtz,[2,‡] and K. O. H. Ziock[1]

[1]*Department of Physics, University of Virginia, Charlottesville, Virginia 22904-4714, USA*
[2]*Paul Scherrer Institute, Villigen PSI, CH-5232, Switzerland*
[3]*Joint Institute for Nuclear Research, RU-141980 Dubna, Russia*
[4]*Institute for Nuclear Studies, PL-05-400 Swierk, Poland*
[5]*Institute for High Energy Physics, Tbilisi State University, GUS-380086 Tbilisi, Georgia*
[6]*Department of Physics and Astronomy, Arizona State University, Tempe, Arizona 85287-1504, USA*
[7]*Rudjer Bošković Institute, HR-10000 Zagreb, Croatia*

(Received 17 December 2003; published 25 October 2004)

We have studied radiative pion decays $\pi^+ \to e^+ \nu\gamma$ in three broad kinematic regions using the PIBETA detector and a stopped pion beam. Based on Dalitz distributions of 41 601 events we have evaluated absolute $\pi \to e\nu\gamma$ branching ratios in the three regions. Minimum χ^2 fits to the integral and differential (E_{e^+}, E_γ) distributions result in the axial-to-vector weak form factor ratio of $\gamma \equiv F_A/F_V = 0.443(15)$, or $F_A = 0.0115(4)$ with $F_V = 0.0259$. However, deviations from standard model predictions in the high-E_γ–low-E_{e^+} kinematic region indicate the need for further theoretical and experimental work.

DOI: 10.1103/PhysRevLett.93.181804 PACS numbers: 13.20.Cz, 11.30.Rd, 14.40.Aq

In the standard model description of radiative pion decay $\pi^+ \to e^+ \nu\gamma$ (also denoted $\pi_{e2\gamma}$), where γ is a real or virtual photon (e^+e^- pair), the decay amplitude M depends on the vector V and axial-vector A weak hadronic currents [1]. Both currents contribute to the structure-dependent terms SD_V and SD_A associated with virtual hadronic states, while only the axial-vector current contributes to the inner bremsstrahlung (IB) process. The structure-dependent amplitude is parametrized by the vector and axial-vector form factors, F_V and F_A [1]. The conserved vector current (CVC) hypothesis [2,3] relates F_V to the π^0 lifetime, yielding $F_V = 0.0259(5)$ [4], which agrees with the relativistic quark model and chiral perturbation theory [5]. Chiral symmetry calculations [5–7] give F_A in the range 0.010–0.014.

The combined $\pi \to e\nu\gamma$ event count of all previously published experiments is less than 1200 events, while the overall uncertainties of the parameter $\gamma \equiv F_A/F_V$ extracted from data range from 12% to 56% [8–13].

In this Letter, we present a first analysis of the $\pi^+ \to e^+ \nu\gamma$ events recorded with the PIBETA detector in the course of a new measurement of the $\pi^+ \to \pi^0 e^+ \nu$ (π_β) branching ratio [14,15] from 1999 to 2001.

The measurements were performed in the πE1 channel at the Paul Scherrer Institute, Villigen, Switzerland, using a stopped π^+ beam and the PIBETA detector. A total of 2.2×10^{13} π^+ stops were recorded during the running period. The main component of the PIBETA detector system is a spherical pure-CsI electromagnetic shower calorimeter. Details of the detector design and performance and of our experimental method are presented at the experiment Web site [16] and in Refs. [15,17].

Two sets of fast analog triggers accepted nearly all nonprompt pion decay events and a substantial fraction of muon decays, for energy depositions in the PIBETA shower calorimeter exceeding a high threshold of HT $\simeq$ 51.7 MeV, or a low threshold of LT $\simeq$ 4.5 MeV. Charged particles emanating from the target were tracked by two cylindrical multiwire proportional chambers [18] and a 20-piece thin plastic-scintillator veto (PV) hodoscope. The PV signals provided discrimination between the background protons and minimum ionizing particles (MIPs). MIP detection efficiencies were continuously monitored; their average values over the entire data sample were $\epsilon_{C1} = 93.7\%$, $\epsilon_{C2} = 97.9\%$, and $\epsilon_{PV} = 98.9\%$, for the two chambers and the PV, respectively. The overall inefficiency for distinguishing neutral and charged particles was therefore 1.5×10^{-5}.

Candidate $\pi \to e\nu\gamma$ events were selected from the two-arm HT and prescaled one-arm HT data sets by requiring one neutral shower in the calorimeter in coincidence with a positron track. In less than 5% of events there was more than one possible coupling (i.e., more than one neutral shower or positron track); the pair most nearly coincident in time was chosen. Our data set covers three kinematic regions: A: $E^{\rm cal}_{e^+}, E^{\rm cal}_\gamma > 51.7$ MeV (two-arm HT); B: $E^{\rm cal}_{e^+} > 20.0$ MeV, $E^{\rm cal}_\gamma > 55.6$ MeV (one-arm HT); C: $E^{\rm cal}_{e^+} > 55.6$ MeV, $E^{\rm cal}_\gamma > 20.0$ MeV (one-arm HT). The superscript "cal" refers to values measured in the CsI calorimeter. In all three regions the relative angle $\theta^{\rm cal}_{e^+\gamma} > 40.0°$.

The peak-to-background ratios P/B are shown in Fig. 1 where the time differences between the radiative

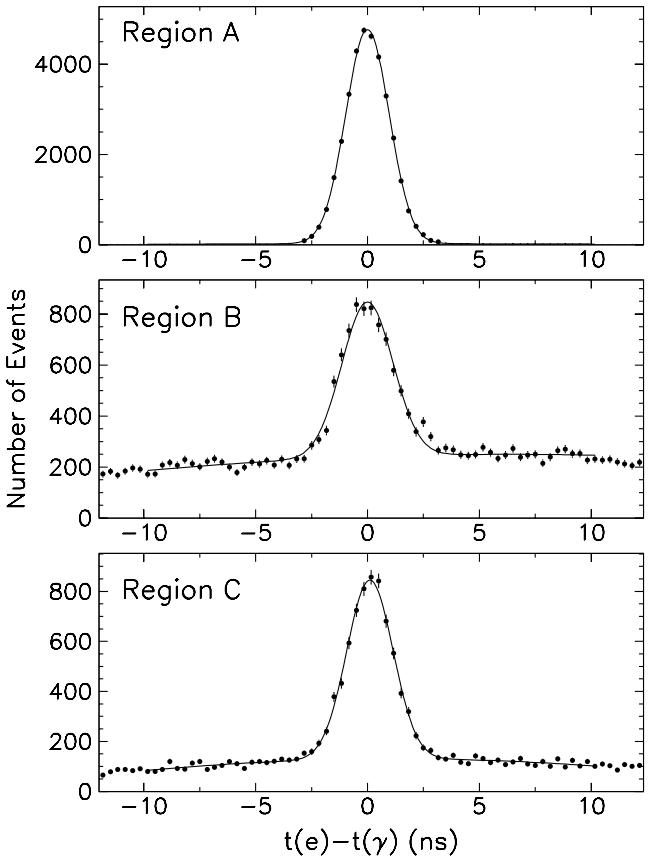

FIG. 1. The region A two-arm trigger $\pi^+ \to e^+\nu\gamma$ events (top panel) are virtually background-free (save for the π_β contamination). The peak-to-background ratios for one-arm trigger region B and region C events are 3.8:1 and 7.6:1, respectively. Solid lines represent Gaussian fits to the peaks.

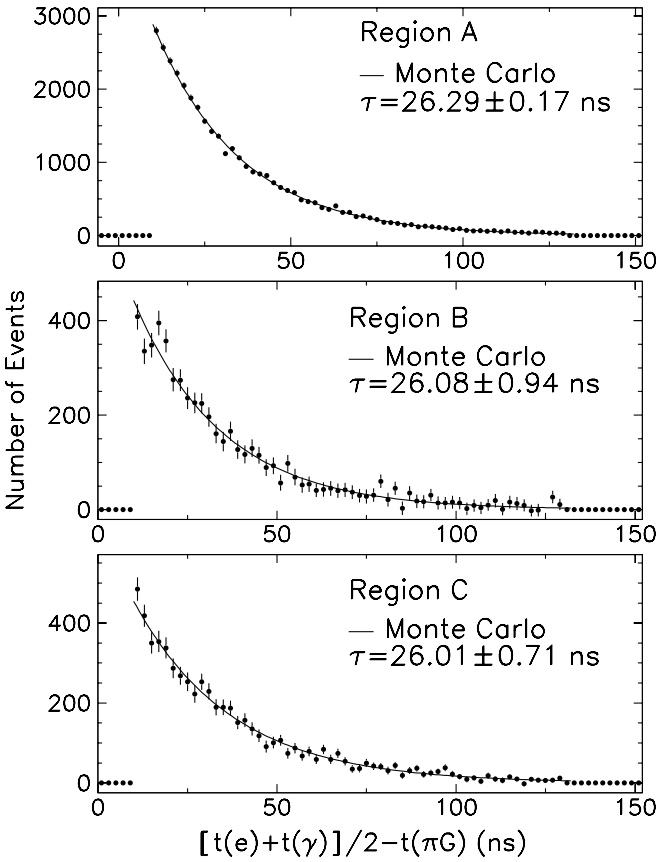

FIG. 2. $\pi^+ \to e^+\nu\gamma$ event timing relative to the π^+ stop gate time, $t(\pi\mathrm{G})$, after accidental background subtraction. Monte Carlo decay functions are shown as solid lines; best-fit values for the pion lifetime are indicated for each region.

photon and the positron tracks are histogrammed. The high energy pairs of region A show virtually no background ($P/B \geq 300$), while the region B (C) events with lower energy positrons (photons) have $P/B = 3.8$ (7.6).

We define the coincidence time window by $\Delta t_{\mathrm{in}} \equiv |t_{e^+} - t_\gamma| \leq 5$ ns. The accidental background was sampled in two sidebands Δt_{out}, $-10\ \mathrm{ns} < t_{e^+} - t_\gamma < -5$ ns and $5\ \mathrm{ns} < t_{e^+} - t_\gamma < 10$ ns. The accidental background, dominated by positrons from the $\pi \to e\nu$ or the π-μ-e decay chain, accompanied by an unrelated neutral shower, was removed by subtracting histograms of observables projected using the out-of-time cut Δt_{out} from the in-time histograms projected via the Δt_{in} cut.

In addition to shower energies, we also measured the directions of the positron and photon, thus overdetermining the final three-body state. The positron direction was fixed using multiwire proportional chamber hits, while the photon direction was reconstructed from the pattern of hits in the calorimeter. Events with kinematics incompatible with the $\pi \to e\nu\gamma$ decay were rejected in the final data sample.

The time distributions of the $\pi \to e\nu\gamma$ events with respect to the π^+ stop time are plotted in Fig. 2. The predicted decay curves are consistent with the π^+ lifetime and demonstrate the purity of the final data set.

Nonaccidental background sources are (1) π_β events for which one π^0 decay photon converts in the target, producing a charged track in the detector, and (2) two-clump showers originating from a single $\pi \to e\nu$ positron when a secondary shower photon or positron interacts in the calorimeter far enough from the primary hit to appear as a separate clump ("split-clump" events).

Starting from the measured net yield of the π_β decay events, we have used the Monte Carlo (MC) simulation of γ conversions in the inner detector to determine that class (1) background events contribute 12.9% of the signal in the kinematic region A and 4.3% (3.8%) in region B (C). These π_β contaminations were subtracted in the calculation of $\pi \to e\nu\gamma$ yields. For the clump energy threshold $E^{\mathrm{cal}}_{e^+,\gamma} > 20.0$ MeV used in the analysis the split-clump background (2) can be neglected.

We have normalized the radiative pion decay rate to the total branching ratio of the $\pi \to e\nu$ (also known as π_{e2}) events, which were recorded in parallel using the prescaled one-arm calorimeter trigger. This procedure assures that most factors in the normalization, including the total number of decaying π^+'s and the combined tracking

efficiency of e^+'s, largely cancel out. The energy spectrum of the $\pi^+ \to e^+\nu$ positrons, shown in Fig. 3, illustrates the accuracy with which we measure that decay. As an independent check of the absolute normalization, we have evaluated the π_{e2} branching ratio from our data and found it to be in agreement with the world average [4] within $<1\%$.

The absolute branching ratio for the $\pi^+ \to e^+\nu\gamma$ decay can be calculated from the expression

$$R_{\pi e2\gamma} = \frac{N_{\pi e2\gamma} p_{\pi e2\gamma}}{N_{\pi^+} g_\pi A_{\pi e2\gamma} \tau_l \epsilon_{\rm PV} \epsilon_{\rm C1} \epsilon_{\rm C2}}, \quad (1)$$

where $N_{\pi e2\gamma}$ is the number of the detected $\pi \to e\nu\gamma$ events, $p_{\pi e2\gamma}$ is the corresponding prescaling factor (if any), N_{π^+} is the number of the decaying π^+'s, $g_\pi = \int_{t_1}^{t_2} \exp(-t/\tau_{\pi^+})dt$ is the π^+ gate fraction, $A_{\pi e2\gamma}$ is the detector acceptance incorporating the appropriate cuts, and τ_l is the detector live time fraction. An analogous expression can be written for the total $R_{\pi e2}$ branching ratio. Combining the two, we obtain

$$R_{\pi e2\gamma} = R_{\pi e2} \frac{N_{\pi e2\gamma} p_{\pi e2\gamma}}{N_{\pi e2} p_{\pi e2}} \frac{A_{\pi e2}}{A_{\pi e2\gamma}} \frac{\epsilon_{\pi e2}}{\epsilon_{\pi e2\gamma}}, \quad (2)$$

where the ϵ's denote the properly weighted products of $\epsilon_{\rm PV}\epsilon_{\rm C1}\epsilon_{\rm C2}$ for the two data sets. The detector acceptance ratio takes on values between 0.057 and 0.209, depending on the kinematic region.

The experimental acceptances depend on both the detector response and the decay amplitudes and are calculated in a MC simulation. The GEANT3 [19] simulation of the PIBETA detector response included (i) the detailed geometry of the active detectors and the passive support material, (ii) the measured detector energy and timing responses, (iii) event generators for π and μ decays including measured accidental pileup rates, and (iv) the photo-absorption reactions in the CsI calorimeter incorporated in the GEANT code.

In the standard model the differential rate of the $\pi^+ \to e^+\nu\gamma$ decay can be written in the form [1]

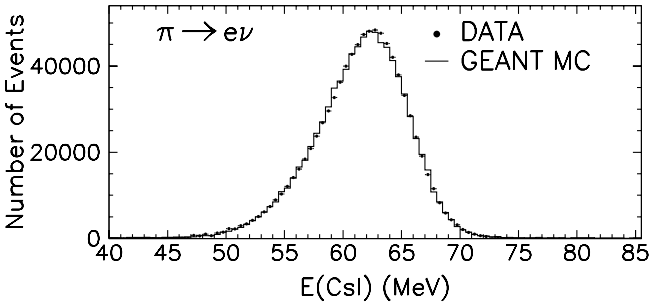

FIG. 3. Background-subtracted $\pi^+ \to e^+\nu$ energy spectrum taken with the one-arm trigger. The GEANT-simulated detector response is represented by the solid line histogram.

$$\frac{d\Gamma_{\pi e2\gamma}}{dxdy} = \frac{\alpha}{2\pi}\Gamma_{\pi e2}\Big\{{\rm IB}(x,y) + \left(\frac{F_V m_\pi^2}{2 f_\pi m_e}\right)^2 [(1+\gamma)^2 {\rm SD}^+(x,y) + (1-\gamma)^2 {\rm SD}^-(x,y)] + \left(\frac{F_V m_\pi}{f_\pi}\right)[(1+\gamma) S^+_{\rm int}(x,y) + (1-\gamma) S^-_{\rm int}(x,y)]\Big\}, \quad (3)$$

where the IB, $\rm SD^\pm$, and $S^\pm_{\rm int}$ (IB-SD interference) terms depend on the kinematic variables $x = 2E_\gamma/m_\pi$ and $y = 2E_e/m_\pi$; E_e and E_γ are the physical ("thrown") energies.

We took the Particle Data Group value $\Gamma(\pi e2)/\Gamma_{\rm total} = 1.230(4) \times 10^{-4}$ [4] and calculated the experimental branching ratios using the MINUIT least chi-square program [20]. We have added integral radiative corrections of -1.0% in region A, -1.4% in B, and -3.3% in C to the theoretical $R_{\rm theor}$'s [21]. The minimization program simultaneously fits two-dimensional $(E^{\rm cal}_{e^+}, E^{\rm cal}_\gamma)$ distributions in all three phase space regions, constraining the integrals to the experimental branching ratio values $(R_{\rm exp})$.

The acceptance $A_{\pi e2\gamma}$ is recalculated in every iteration step of our analysis with the cuts applied to the physical (thrown) energies, E, following cuts applied to measured particle energies and angles, $E^{\rm cal}$, $\theta^{\rm cal}$. Hence, our experimental branching ratios can be compared directly with theoretical absolute decay rates.

The statistical uncertainties of the experimental yields are 0.6% (30 670 events, region A), 1.7% (5233 events, region B), and 1.5% (5698 events, region C). Systematic uncertainties of 1.8% for region A, dominated by π_β background subtraction, 2.3% and 3.1% for regions B and C, respectively, both dominated by acceptance uncertainties, were added in quadrature.

The dependence of the region A experimental and theoretical branching ratio on the value of γ is shown in Fig. 4 (top panel), indicating two solutions. The positive γ solution is preferred by a χ^2 ratio of $\sim$50:1 once data from regions B and C are included in the analysis (bottom panel). We compare the experimental and theoretical branching ratios for the three phase space regions in Table I. We note that, due to the large statistical and systematic uncertainties present in all older experiments, our values are consistent with previously published measurements. The best CVC fit to our data yields $\gamma = 0.443 \pm 0.015$, or $F_A = 0.0115(4)$ with $F_V \equiv 0.0259$. This result represents a fourfold improvement in precision over the previous world average $F_A = 0.0116(16)$ [4]. It is consistent with chiral Lagrangian calculations [5–7] and will lead to a correspondingly improved precision in the order p^4 chiral constant l_{10} [5,22].

In summary, our experimental $\pi^+ \to e^+\nu\gamma$ branching ratios and energy distributions in kinematic regions A and C are compatible with the $(V-A)$ interaction. The sizable 19% shortfall in the measured branching ratio in region B dominates the total χ^2 and is disconcerting. Thus, in a fit

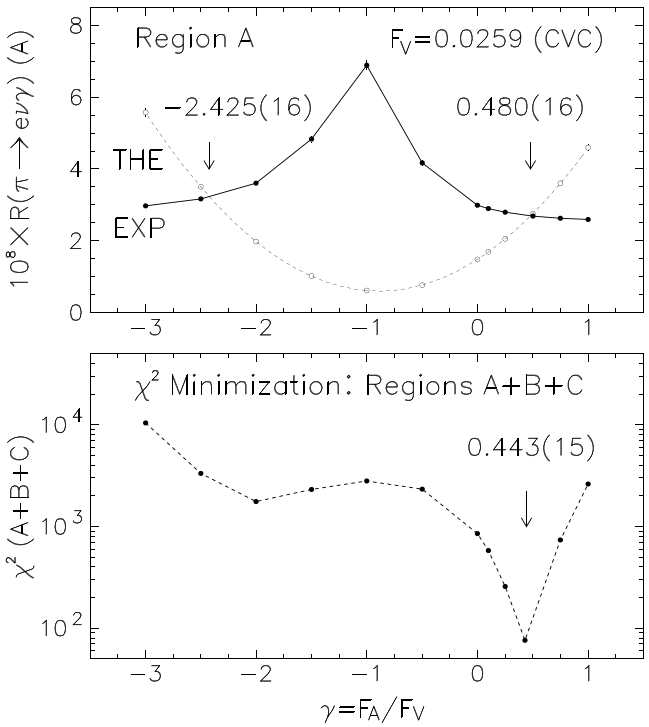

FIG. 4. Top panel: $\pi^+ \to e^+\nu\gamma$ branching ratio values as a function of $\gamma \equiv F_A/F_V$. The theoretical parabola follows from the $V - A$ model, Eq. (3). The experimental values reflect fits to region A data only. Bottom panel: minimum χ^2 values of simultaneous fits to the entire data set (regions A, B, and C).

restricted to region A data only, we obtain $\gamma = 0.480 \pm 0.016$; this result remains unchanged if region C data are added to the fit. Significantly, all previous studies, save one (which, too, found an anomaly) [13], have analyzed only data with kinematics compatible with our region A.

Taking the $(V - A)$ interaction and the CVC hypothesis as valid, the deficit could be caused by a peculiar detection or analysis inefficiency in our experiment, appearing dominantly in region B. Detailed cross-checks, including absolute total and differential $\pi \to e\nu$, $\pi^+ \to \pi^0 e^+ \nu$, $\mu \to e\nu\bar{\nu}$, and $\mu \to e\nu\bar{\nu}\gamma$ branching ratio evaluations in a comprehensive analysis, have rendered such inefficiencies extremely improbable [23].

Alternatively, the deficit could be caused by an inadequacy of the present $V - A$ description of the radiative pion decay, along with the radiative corrections, or by an anomalous, non-$(V - A)$ interaction [13,24–26]. We note that our results clearly call for further theoretical and experimental work.

TABLE I. Best-fit $\pi \to e\nu\gamma$ branching ratios obtained with $F_V = 0.0259$ (fixed) and $F_A = 0.0115(4)$ (fit); $\chi^2/\mathrm{dof} = 25.4$. Measured ($R_{\mathrm{exp}}$) and theoretical ($R_{\mathrm{theor}}$) branching ratios are shown for the three indicated phase space regions. Radiative corrections are included in the calculations.

$E_{e^+}^{\mathrm{min}}$ (MeV)	E_γ^{min} (MeV)	$\theta_{e\gamma}^{\mathrm{min}}$	R_{exp} ($\times 10^{-8}$)	R_{theor} ($\times 10^{-8}$)
50	50	none	2.71(5)	2.583(1)
10	50	40°	11.6(3)	14.34(1)
50	10	40°	39.1(13)	37.83(1)

We thank W. Stephens and Z. Hochman for invaluable help in preparing and running the experiment. We thank M. Chizhov and A. Poblaguev for fruitful discussions and comments, as well as E. Kuraev and Yu. Bystritsky for communicating to us their radiative correction results prior to publication. The PIBETA experiment has been supported by the U.S. National Science Foundation, U.S. Department of Energy, the Paul Scherrer Institute, and the Russian Foundation for Basic Research.

*Corresponding author.
Electronic address: frlez@virginia.edu
†Corresponding author.
Electronic address: pocanic@virginia.edu
‡Present address: Philips Semiconductors AG, CH-8045 Zürich.

[1] D. A. Bryman *et al.*, Phys. Rep. **88**, 151 (1982).
[2] S. S. Gershtein and I. B. Zel'dovich, Zh. Eksp. Teor. Fiz. **29**, 698 (1955) [Sov. Phys. JETP **2**, 576 (1956)].
[3] R. P. Feynman and M. Gell-Mann, Phys. Rev. **109**, 193 (1958).
[4] Particle Data Group, S. Eidelman *et al.*, Phys. Lett. B **592**, 1 (2004).
[5] C. Q. Geng *et al.*, Nucl. Phys. **B684**, 281 (2004).
[6] B. R. Holstein, Phys. Rev. D **33**, 3316 (1986).
[7] J. Bijnens and P. Talavera, Nucl. Phys. **B489**, 387 (1997).
[8] P. Depommier *et al.*, Phys. Lett. **7**, 285 (1963).
[9] A. Stetz *et al.*, Nucl. Phys. **B138**, 285 (1978).
[10] A. Bay *et al.*, Phys. Lett. B **174**, 445 (1986).
[11] L. E. Piilonen *et al.*, Phys. Rev. Lett. **57**, 1402 (1986).
[12] C. A. Dominguez and J. Solc, Phys. Lett. B **208**, 131 (1988).
[13] V. N. Bolotov *et al.*, Phys. Lett. B **243**, 308 (1990).
[14] D. Počanić *et al.*, Paul Scherrer Institute Experiment Proposal No. PSI R-89.01, 1992.
[15] D. Počanić *et al.*, Phys. Rev. Lett. **93**, 181803 (2004).
[16] $\pi\beta$ home page, http://pibeta.phys.virginia.edu.
[17] E. Frlež *et al.*, Nucl. Instrum. Methods Phys. Res., Sect. A **526**, 300 (2004).
[18] V.V. Karpukhin *et al.*, Nucl. Instrum. Methods Phys. Res., Sect. A **418**, 306 (1998).
[19] R. Brun *et al.*, computer code GEANT 3.21, CERN, Geneva, 1994.
[20] F. James and M. Roos, computer code MINUIT 94.1, CERN, Geneva, 1989.
[21] E. A. Kuraev and Y. M. Bystritsky, Phys. Rev. D **69**, 114004 (2004).
[22] G. Amoros *et al.*, Nucl. Phys. **B602**, 87 (2001).
[23] PIBETA Collaboration, E. Frlež *et al.*, hep-ex/0312025.
[24] P. Herczeg, Phys. Rev. D **49**, 247 (1994).
[25] A.V. Chernyshev *et al.*, Mod. Phys. Lett. A **12**, 1669 (1997).
[26] M.V. Chizhov, Mod. Phys. Lett. A **8**, 2753 (1993).